Synthesis and Characterization of More Potent Analogues of Hirudin Fragment 1−47 Containing Non-Natural Amino Acids[†,‡]

Vincenzo De Filippis,[§] Daniela Quarzago,[§] Alessandro Vindigni,[||] Enrico Di Cera,[||] and Angelo Fontana*[,§]

CRIBI Biotechnology Centre, University of Padua, Via Trieste 75, 35131 Padua, Italy, and Department of Biochemistry and Molecular Biophysics, Washington University School of Medicine, St. Louis, Missouri 63110

Received March 30, 1998; Revised Manuscript Received June 22, 1998

ABSTRACT: Hirudin is the most potent and specific inhibitor of thrombin, a key enzyme in the coagulation process existing in equilibrium between its procoagulant (fast) and anticoagulant (slow) form. In a previous study, we described the solid-phase synthesis of a Trp3 analogue of fragment 1−47 of hirudin HM2, which displayed ∼5-fold higher thrombin inhibitory potency relative to that of the natural product [De Filippis, V., et al. (1995) *Biochemistry 34*, 9552−9564]. By combining automated and manual peptide synthesis, here we have produced in high yields seven analogues of fragment 1−47 containing natural and non-natural amino acids. In particular, we have replaced Val1 with *tert*-butylglycine (*t*Bug), Ser2 with Arg, and Tyr3 with Phe, cyclohexylalanine (Cha), Trp, α-naphthylalanine (αNal), and *β*-naphthylalanine (*β*Nal). The crude reduced peptides are able to fold almost quantitatively into the disulfide-cross-linked species, whose unique alignment (Cys6-Cys14, Cys16-Cys28, and Cys22-Cys37) has been shown to be identical to that of the natural fragment. The results of conformational characterization provide evidence that synthetic peptides retain the structural features of the natural species, whereas thrombin inhibition data indicate that the synthetic analogues are all more potent inhibitors of thrombin. In particular, Val → *t*Bug exchange leads to a 3-fold increase in binding, interpreted as arising from a favorable reduction of the entropy of binding, due to the presence of the more symmetric side chain of *t*Bug relative to that of Val. The S2R analogue binds 24- and 125-fold more tightly than the natural fragment to the fast or slow form of thrombin. These results are explained by considering that Arg2 may favorably couple to Glu192, a key residue involved in the slow to fast transition, thus stabilizing the slow form. Replacement of Tyr3 with more hydrophobic residues having different side chain orientations and electronic structures improves binding by 2−40-fold, suggesting that nonpolar interactions and shape-dependent packing effects strongly influence binding at this position. Overall, these results provide new insights for elucidating the mechanism of hirudin−thrombin recognition at the molecular level and highlight new strategies for designing more potent and selective inhibitors of thrombin.

Thrombin is a key enzyme in the coagulation cascade (*1*) and accomplishes two opposite roles in hemostasis. The procoagulant role entails conversion of fibrinogen into fibrin and enhancement of its own production from prothrombin through feedback activation of proteases upstream in the coagulation cascade. The anticoagulant role encompasses activation of protein C through site-specific proteolysis. Activated protein C rapidly inactivates factors Va and VIIIa, both of which are involved in thrombin generation (*2*). It has been recently demonstrated that thrombin is an allosteric enzyme existing in two conformations, the slow and fast forms (*3*). The fast form exerts a procoagulant activity by specifically cleaving fibrinogen into fibrin, while the slow form is anticoagulant since it specifically activates protein C (*4*). The slow to fast transition is triggered by Na^+ binding to a site located in the loop connecting the last two *β*-strands of the B-chain of thrombin (*5*). Under physiological conditions of Na^+ concentration, temperature, and pH, the slow and fast forms are almost equally populated (*3*) so the procoagulant and anticoagulant activities of thrombin that are crucial for effective hemostasis are balanced. In this respect, the possibility of indentifying molecules that modulate the procoagulant and anticoagulant activities of thrombin is an attractive strategy for developing novel anticoagulant agents (*6*).

Hirudin is the most potent and specific inhibitor of thrombin, with a dissociation constant of 22 fM (*7*). NMR studies conducted on hirudin HV1[1] (*8*, *9*) and HM2 (*10*) variants show that hirudin is composed of a compact N-terminal region cross-linked by three disulfide bridges and a flexible negatively charged C-terminal tail. The high-resolution X-ray structure of the hirudin−thrombin complex indicates that the N-terminal domain of hirudin binds to the active site, while the C-terminal tail binds through electrostatic interactions to the fibrinogen-binding site (exosite I)

[†] This work was supported by the Italian National Council of Research (CNR), by the Ministry of University and Research (MURST), and by NIH Grants.

[‡] Part of this study was presented at the second European Symposium of the Protein Society, Cambridge (U.K.), April 12−16, 1997 (communication 283).

* To whom correspondence should be addressed. Telephone: +39-49-827-6156. Fax: +39-49-827-6159. E-mail: fontana@civ.bio.unipd.it.

[§] University of Padua.

[||] Washington University School of Medicine.

S0006-2960(98)00717-X CCC: $15.00
Published on Web 09/05/1998

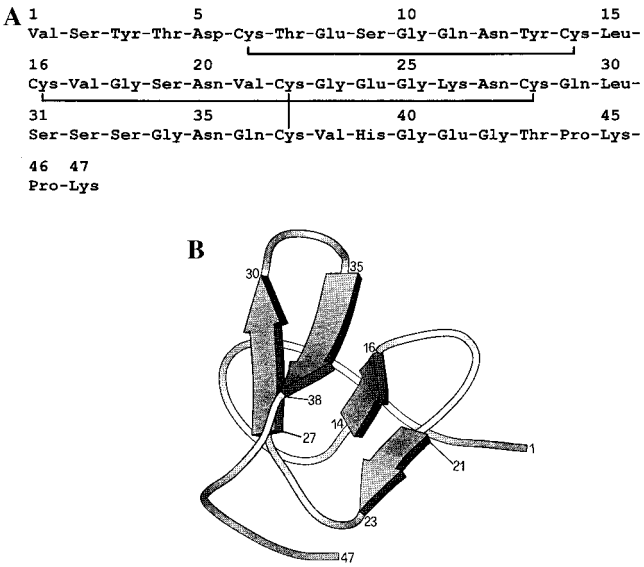

FIGURE 1: (A) Amino acid sequence of the N-terminal fragment 1−47 of hirudin HM2 from *H. manillensis* (*58*). The three disulfide bridges between residues 6 and 14, 16 and 28, and 22 and 37 are indicated by plain lines. (B) Schematic representation of the model structure of natural fragment 1−47 of hirudin HM2. The model is based on the coordinates of the NMR solution structure of the homologous HV1 variant from *H. medicinalis* (*8*; PDB entry code 5HIR). Ribbons with arrows indicate β-strands and rope loop regions. Numbers define amino acid segments in the β-structure. The ribbon drawing was generated using the program Molscript (*59*).

on thrombin (*11*, *12*). Interestingly, either fragment 1−49 and full-length hirudin HV1 bind ∼30 times more tightly to the fast form of thrombin than to the slow form (*13*), suggesting that the structural determinants of this preferential binding reside in the N-terminal domain.

Much effort has been put forth to produce hirudin analogues displaying more potent antithrombin activity by using genetic methods (*14*−*17*). Special attention was also devoted to the chemical synthesis of divalent thrombin inhibitors, hirulogs (*18*), and hirunorms (*19*), based on the C-terminal sequence of residues 55−65 of hirudin. Both hirulogs and hirunorms bind through their N-terminal segment to the active site of thrombin and through the C-terminal tail to exosite I.

In a previous paper, we described the chemical synthesis of a Trp3 analogue of fragment 1−47 of hirudin HM2 from *Hirudinaria manillensis* (see Figure 1) displaying ∼5-fold higher thrombin inhibitory potency (*20*). In this study, we extend the chemical and analytical methods previously developed to further elucidate the mechanism of molecular recognition between hirudin and thrombin. Taking advantage of the versatility of solid-phase synthesis, we have produced in high yields seven analogues of fragment 1−47 of hirudin HM2 containing natural (Arg, Phe, and Trp) and non-natural (*tert*-butylglycine, cyclohexylalanine, and α- and β-naphthylalanine) amino acid residues at the level of the N-terminal tripeptide (Figure 2). The inhibitory activities of the synthetic analogues toward the slow and fast forms of thrombin were compared to that of the natural species and interpreted on the basis of the different physicochemical properties of the mutated residues.

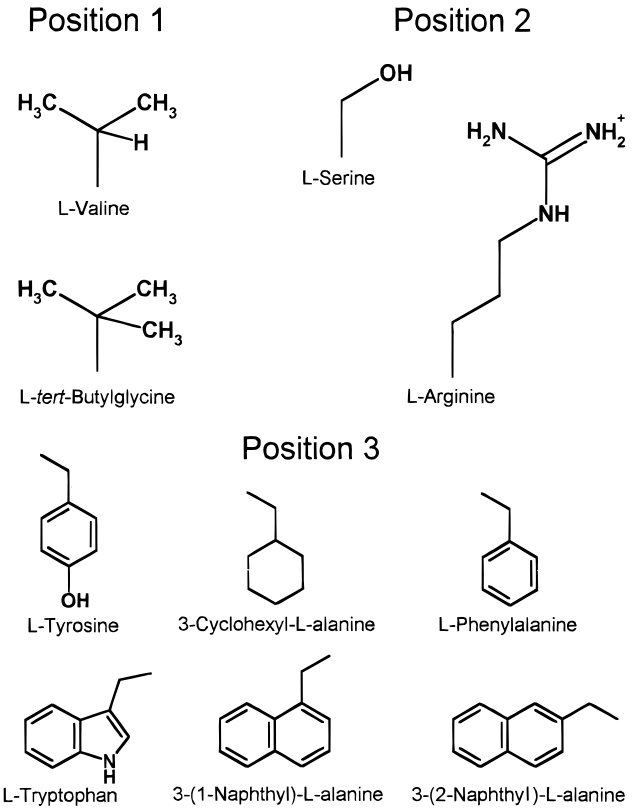

FIGURE 2: Chemical structure of the amino acid side chains of the natural fragment 1−47 and of its synthetic analogues at positions 1−3 (see Figure 1).

Amino Acid Replacements

The X-ray structure of the complex of bovine and human α-thrombin with the hirudin HV1 or HV2 variant (*11*, *12*) indicates that the three N-terminal residues of hirudin are completely buried in the active site of the enzyme and form a parallel β-sheet with Ser214−Gly219 of thrombin. Moreover, the N-terminal tripeptide makes about half of the total contacts observed for the binding of the N-terminal core domain 1−49 to thrombin (*11*) and accounts for ∼30% of the total free energy of binding (*17*). Hence, the first three amino acid residues of hirudin represent a suitable target for quantitative studies of hirudin recognition by thrombin.

Val1. The N-terminal end of hirudin is very sensitive to structural modifications. Acetylation or addition of an extra Gly residue at the N-terminal α-amino group almost abolishes the anti-thrombin activity of hirudin (*14*), while substitution of Val1 with neutral (Gly) or polar (Ser, Glu, or Lys) residues decreases binding by 10−1200-fold, respectively (*17*). NMR studies conducted on the hirudin HV1

[1] Abbreviations: ASA, accessible surface area; CD, circular dichroism; ChCl, choline chloride; EDT, ethanedithiol; Fmoc, 9-fluorenylmethyloxycarbonyl; HBTU, 2-(1*H*-benzotriazol-1-yl)-1,1,3,3-tetramethyluronium hexafluorophosphate; HOBt, 1-hydroxybenzotriazole; HPLC, high-pressure liquid chromatography; PEG, poly(ethylene glycol); RP, reverse-phase; TFA, trifluoroacetic acid; UV, ultraviolet; HM2 and HV1, hirudin variants isolated from the leeches *Hirudinaria manillensis* and *Hirudo medicinalis*, respectively; V1*t*Bug, synthetic analogue of fragment 1−47 of hirudin HM2 in which Val1 has been replaced by *tert*-butylglycine (*t*Bug); S2R, mutation of Ser2 with Arg; Y3F and Y3W, sequence 1−47 of hirudin HM2 in which Tyr3 has been replaced by Phe and Trp, respectively; Y3Cha, Y3αNal, and Y3βNal, analogues obtanined by replacing Tyr3 with cyclohexylalanine (Cha), α-naphthylalanine (αNal), and β-naphthylalanine (βNal), respectively.

(*8*, *9*, *21*, *22*) and HM2 variant (*10*) indicate that Val1 (present in both isoforms) is almost fully exposed to solvent and highly flexible. Conversely, in the bound state, Val1 is completely buried in the active site of the enzyme and fixed in a single side chain conformation (*11*, *12*). In particular, the α-NH_2 group of Val1 forms a hydrogen bond with Oγ of the catalytic Ser195, while its side chain makes numerous hydrophobic contacts with His57 of the catalytic triad and closely interacts with Tyr60A and Trp60D of the 60A−I insertion loop. This loop, absent in other homologous trypsin-like proteases, defines the S2 specificity site on thrombin and narrows the access to the active site such that only small apolar residues are allowed.

Considering the structural properties of hirudin in the free and bound state and the steric requirements at the S2 site of thrombin, we replaced Val1 with *tert*-butylglycine (*t*Bug) (see Figure 2). In fact, both Val and *t*Bug have comparable side chain volumes (*23*), disfavor helix formation (*24*, *25*), and have strong β-forming propensities (*26*, *27*), with minimum energy points at $\phi,\psi = -90°,100°$ for Val and $\phi,\psi = -130°,140°$ for *t*Bug (*26*). On the other hand, the addition of a methyl group to Cβ of valine is expected to restrict the backbone conformations available to *t*Bug to about one-third of those allowed to Val (*26*).

Ser2. Mutagenesis studies conducted on the hirudin HV1 variant indicate that substitution of Val2 with Arg leads to a 9-fold improved binding (*17*). Analysis of the three-dimensional (3D) structure of the hirudin−thrombin complex reveals that position 2 of hirudin is located at the entrance to, but does not enter, the S1 site, formed by two large loops comprising Cys182−Ser195 and Val213−Tyr228 (*11*). Hence, the occupancy of the S1 site is not strictly required for binding. The improved binding of the Val2Arg mutant in hirudin HV1 was interpreted by considering that the side chain of Arg is long enough to favorably interact with Asp189 at the bottom of the S1 site of thrombin. However, alternative binding modes implying interaction of Arg2 with Glu192 or Asp194 thereby were not excluded (*17*). Here we have replaced Ser2 with Arg to evaluate the effects of perturbation of the S1 site on the binding efficiency of hirudin fragment 1−47 to the slow and fast forms of thrombin.

Tyr3. Contrary to the high conformational flexibility observed for the first two residues of hirudin, Tyr3 has a well-defined conformation both in the free and in the bound state (*10*−*12*, *21*). In the hirudin−thrombin complex, the side chain of Tyr3 projects into the apolar binding site of thrombin (the S3 site), formed by a large hydrophobic cavity comprising residues Trp215, Leu99, and Ile174 (*11*). The importance of position 3 is confirmed by the fact that Tyr3 is highly conserved through the hirudin family (*28*), and its substitution or chemical modification significantly affects thrombin binding. In particular, Tyr → Ala exchange and nitration of Tyr3 dramatically reduce binding (*16*, *17*). On the other hand, replacement of Tyr3 in hirudin HV1 with the more hydrophobic Phe and Trp improves binding (*15*). Similar results were obtained with fragment 1−47 of hirudin HM2, where Tyr3 → Trp exchange led to a 5-fold increase in binding (*20*). Conversely, chemical modification of Trp3 with the bulky and hydrophobic *o*-nitrophenylsulfenyl (NPS) group almost abolishes the affinity for thrombin, suggesting that the molecular shape and steric hindrance at position 3 are crucially important for binding (*29*).

To probe the S3 site of thrombin, we have replaced Tyr3 with natural (Phe and Trp) and non-natural (Cha, αNal, and βNal) amino acids (see Figure 2). Since these residues are all more hydrophobic than Tyr, as seen in water → octanol transfer data (*23*), and display different physicochemical properties, it is possible to produce hirudin fragments 1−47 with relatively large structural and chemical diversity at position 3 (i.e., hydrophobicity, electronic structure, side chain volume, and orientation).

MATERIALS AND METHODS

Fragment 1−47 of hirudin from *H. manillensis* (variant HM2) was obtained by limited proteolysis with trypsin of the 64-residue chain of hirudin HM2 (*30*). Human α-thrombin (EC 3.4.21.5) was purified and tested for activity as described previously (*3*). The chromogenic substrate D-Phe-Pro-Arg-*p*-nitroanilide (FPR) was synthesized by the liquid-phase method. Fmoc derivatives of the non-natural amino acids reported in this work were prepared using the method previously described (*31*). Protected amino acids, solvents, and reagents for peptide synthesis, as well as those for peptide and/or protein sequence analysis, were from Applied Biosystems (Foster City, CA). Cyclohexylalanine (Cha), *tert*-butylglycine (*t*Bug), α-naphthylalanine (αNal), and β-naphthylalanine (βNal) were purchased from Sigma (St. Louis, MO). Trifluoroacetic acid (TFA) and phenyl isothiocyanate (PITC) were purchased from Pierce (Rockford, IL); poly(ethylene glycol) (PEG) 6000 and dithiothreitol (DTT) were from Fluka (Basel, Switzerland). All other reagents and organic solvents were of analytical grade and obtained from Fluka or Merck (Darmstadt, Germany).

Peptide Synthesis. The analogues of fragment 1−47 of hirudin HM2 were synthesized by the solid-phase Fmoc method (*32*) in two sequential steps. In the first step, the peptide chain corresponding to the sequence of residues 4−47 was assembled stepwise using an Applied Biosystems automated peptide synthesizer (model 431) on a *p*-alkoxybenzyl ester polystyrene resin (0.52 g, 1% divinylbenzene cross-linked) (*33*) derivatized with Fmoc-Lys (0.48 mequiv/g). After the assembly of the peptide chain of residues 4−47 was completed, the side chain-protected peptidyl resin (1.8 g, ∼0.14 mmol of peptide) with the N^{α}-Fmoc protecting group still bound was divided into aliquots (220 mg, ∼20 μmol). Thereafter, the N^{α}-Fmoc was removed, and the coupling of the remaining amino acids was accomplished by manual chemical synthesis, using essentially the same protocol that was used for the automated synthetic procedure. The coupling reaction was performed with the HBTU/HOBt acivation procedure (*34*), using a 4-fold molar excess of protected amino acids. A double-coupling cycle was required only for the incorporation of the sterically hindered *tert*-butylglycine (*t*Bug) at the N terminus. After the assembly of the analogues of hirudin fragment 1−47 was completed, the side chain-protected peptidyl resin was treated for 90 min at 0 °C with a 2 mL mixture of TFA/H_2O/EDT (95:2.5:2.5, v/v). In the case of the S2R analogue, a 4 h TFA treatment was used to maximize deprotection of the Mtr group (4-methoxy-2,3,6-trimethylbenzenesulfonyl) from the Arg side chain (*32*). The crude reduced peptide was dissolved (2 mg/mL) in 0.1 M $NaHCO_3$ buffer (pH 8.3) and allowed to fold for 24 h under air oxidation conditions in the presence of 100 μM β-mercaptoethanol (*35*). The

refolding mixture was fractionated using an analytical Vydac (The Separations Group, Hesperia, CA) C18 column (4.6 mm × 150 mm, 5 μm particle size) eluted with a linear acetonitrile/0.05% TFA gradient. For preparative purposes, aliquots (2−3 mg) of crude refolded peptide were injected onto a semipreparative Vydac C18 column (1 cm × 25 cm, 10 μm particle size). The analytical characterization of the synthetic peptides and the determination of disulfide pairing were conducted as previously described for the Y3W analogue (*20*).

Spectroscopic Measurements. The concentration of the analogues of fragment 1−47 was determined by ultraviolet (UV) absorption at 280 nm on a double-beam model Lambda-2 spectrophotometer from Perkin-Elmer (Norwalk, CT). Extinction coefficients at 280 nm for the natural fragment and for the analogues V1*t*Bug, S2R, Y3Cha, Y3F, and Y3W were calculated utilyzing a molar absorption coefficient of 1280 M^{-1} cm^{-1} for tyrosine, 5690 M^{-1} cm^{-1} for tryptophan, and 120 M^{-1} cm^{-1} for cysteine (*36*), and taken to be 0.67 mg^{-1} cm^2 for the natural fragment 1−47 and for analogues V1*t*Bug and S2R, 0.41 mg^{-1} cm^2 for Y3F and Y3Cha, and 1.57 mg^{-1} cm^2 for the Y3W analogue. The extinction coefficients for the naphthylalanine-containing peptides were obtained by using a molar absorption coefficient of 6200 M^{-1} cm^{-1} for αNal (*37*, *38*) and 5380 M^{-1} cm^{-1} for βNal (*39*), and calculated as 1.67 and 1.50 mg^{-1} cm^2 for Y3αNal and Y3βNal, respectively.

Circular dichroism (CD) spectra were recorded on a Jasco (Tokyo, Japan) model J-710 spectropolarimeter equipped with a thermostated cell holder and a NesLab (Newington, NH) model RTE-110 water circulating bath. Far- and near-ultraviolet CD spectra were recorded at 20 °C in 10 mM phosphate buffer (pH 7.0) at a peptide concentration ranging from 20 to 100 μM, using 1 or 5 mm path length quartz cells in the far- and near-ultraviolet region, respectively.

Fluorescence emission spectra were recorded at 20 °C on a Perkin-Elmer model LS-50B spectrofluorimeter, at a peptide concentration of 5−10 μM in 10 mM phosphate buffer (pH 7.0).

Thrombin Inhibitory Activity. Binding of hirudin N-terminal fragments was quantified from analysis of the competitive inhibition of substrate hydrolysis (*13*, *40*). Measurements were carried out at 25 °C in 5 mM Tris (pH 8.0) containing 0.1% (w/w) PEG 6000. The ionic strength was kept constant at 200 mM with NaCl for the fast form or with ChCl when the slow form was being studied. The active thrombin concentration was 50 pM when the fast form was being studied and 200 pM when the slow form was. The properties of the fast form were derived as the extrapolation at $[Na^+] \rightarrow \infty$ at a constant ionic strength of 200 mM.

Computational Methods. The structure of the synthetic analogues of fragment 1−47 of hirudin HM2 in the free and thrombin-bound state was modeled on the NMR solution structure of hirudin HV1, showing ∼75% sequence homology with hirudin HM2 (*8*; PDB entry code 5HIR), or on the X-ray structure of the hirudin−thrombin complex (*11*; PDB entry code 4HTC), by following essentially the procedure previously described (*30*).

The contribution of hydrophobicity to the free energy change of binding (ΔG_b) was obtained by calculating the difference in the free energy change due to desolvation of polar and apolar groups that are shielded from water upon hirudin−thrombin association (ΔG_{desolv}). An estimate of ΔG_{desolv} is obtained from the equation $\Delta G_{desolv} = -\Sigma_l \Delta\sigma_l \Delta ASA_l$ (*41*, *42*), where ΔASA_l is the change in the accessible surface area (ASA) for atom type 1 upon binding of hirudin analogues to thrombin and $\Delta\sigma_l$, also called the atomic solvation parameter (ASP), is the solvation free energy change per unit area that becomes buried upon binding. ASPs are those reported by Eisenberg and McLachlan (*43*) [$\Delta\sigma$(C) = 16 cal mol^{-1} $Å^{-2}$; $\Delta\sigma$(N/O) = −6 cal mol^{-1} $Å^{-2}$] and are based on water → octanol transfer data for amino acid residues obtained at 25 °C (*23*). ASA calculations were carried out on the natural and synthetic peptide analogues in the free and thrombin-bound state by using the program ACCESS (*44*) and using a probe radius of 1.4 Å.

RESULTS

Synthesis and Characterization. The analogues of fragment 1−47 of hirudin HM2 from *H. manillensis* were obtained by following essentially the procedure previously established for the synthesis of the Y3W analogue (*20*). In all cases, high yields of synthesis (50−60%) were obtained. The crude reduced peptide analogues were allowed to fold for 24 h under air oxidation conditions at pH 8.3 in the presence of β-mercaptoethanol (*35*). The oxidative folding reaction of all the synthetic peptides 1−47 proceeded with an efficiency similar to that observed for the natural fragment and for its Y3W analogue, while the correctness of the disulfide pairing was established by the peptide mapping strategy previously reported (*20*). The homogeneity and chemical identity of the disulfide-oxidized 1−47 analogues were accessed by a number of analytical criteria, including RP-HPLC, capillary zone electrophoresis, amino acid and N-terminal sequence analysis, and electrospray mass spectrometry, giving experimental values consistent with theoretical data (not shown).

Absorption and fluorescence properties of the synthetic 1−47 analogues reflect their specific content of aromatic residues. For instance, the UV absorption and fluorescence emission spectra of Y3αNal are shown in Figure 3. Both spectra are dominated by the contribution of the naphthyl chromophore and are similar to those previously reported for model compounds of αNal (*37*, *38*). Far-UV CD spectra of the synthetic 1−47 analogues share common features of β-like secondary structure (*45*), with a negative absorption centered at 220 nm and an intense positive band at 193 nm (Figure 4A). However, some differences exist between the natural fragment and the synthetic products in terms of both signal intensity and wavelength shift. As previously established for the Y3W analogue (*20*), these differences can be interpreted on the basis of the different contributions of the aromatic chromophores to the CD signal in the far-UV region and not of secondary structure alterations that might have been caused by the mutation that was introduced. Near-UV CD spectra of the synthetic peptide analogues have shape and ellipticity values similar to those of the natural fragment 1−47 (Figure 4B), with a prominent positive absorption at about 260 nm, due to the contribution of disulfide bonds (*46*) and some fine structure in the 280−300 nm region, due to the contribution of the different aromatic residues present

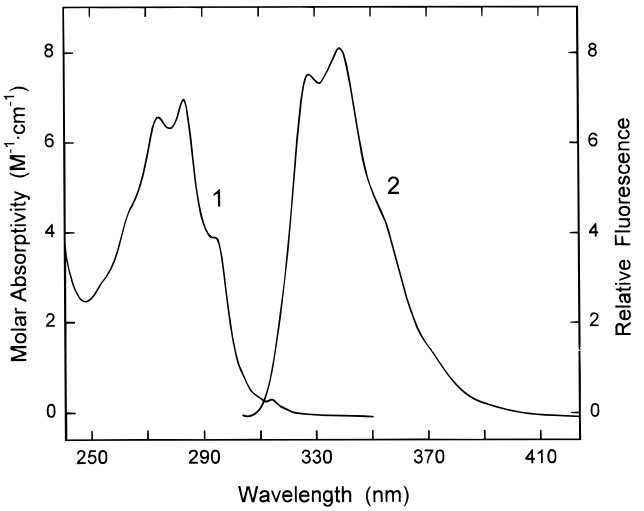

FIGURE 3: Ultraviolet absorption (curve 1) and emission fluorescence spectra (curve 2) of the Y3αNal analogue. Spectra were taken at 20 °C in 10 mM sodium phosphate buffer (pH 7.0) at protein concentrations of 100 and 5 μM for the UV absorption and fluorescence spectra, respectively.

at position 3 (*47*). Moreover, the positive sign and ellipticity values of the 260 nm band indicate that in all the peptide analogues studied the three disulfide bonds are in a right-handed conformation (*46*). This result compares favorably with the NMR solution structure of hirudin (*8*, *10*, *21*, *22*) and with the crystallographic analysis of the hirudin−thrombin complex (*11*). As shown in Figure 4B, the spectrum of V1*t*Bug is almost superimposable with that of the natural fragment 1−47, whereas that of Y3αNal displays some difference in the 270−300 nm region, assigned to the contribution of the naphthyl chromophore. The difference spectra obtained by subtracting the spectrum of Y3Cha from that of Y3αNal or V1*t*Bug (Figure 4, inset) account for the contribution of Tyr (*47*) or αNal (*38*).

Overall, the results of CD measurements lead us to the conclusion that the native fold of hirudin fragment 1−47 is retained upon incorporation of natural (Phe, Trp, and Arg) or non-natural (*t*Bug, Cha, αNal, and βNal) amino acid residues and that the observed differences in the far- and near-UV CD spectra can be ascribed solely to the different intrinsic spectroscopic properties of the mutated residues.

Thrombin Inhibition. Binding of hirudin N-terminal fragments to thrombin was quantified from the analysis of the competitive inhibition of the hydrolysis of the substrate D-Phe-Pro-Arg-*p*-nitroanilide (FPR), as described in Materials and Methods. The relevant properties of the synthetic analogues analyzed in this study are summarized in Table 1. The mutated species display from 2- to 40-fold more potent inhibitory activity toward the fast form of thrombin and up to 125-fold more potent activity toward the slow form, compared to the natural product. In particular, introduction of a methyl group at Cβ of Val1 leads to a 3-fold higher affinity for the fast form, while replacement of Ser2 with Arg enhances binding to the fast and slow form by 24- and 125-fold, respectively. If it is considered that Arg2 may be susceptible to proteolytic attack by thrombin by interacting with its primary specificity site (S1 site) (*48*), a sample of S2R used in the thrombin inhibition assay was recoverd by RP-HPLC and tested for chemical identity. The lack of fragmentation peaks in the RP-HPLC chromatogram and the

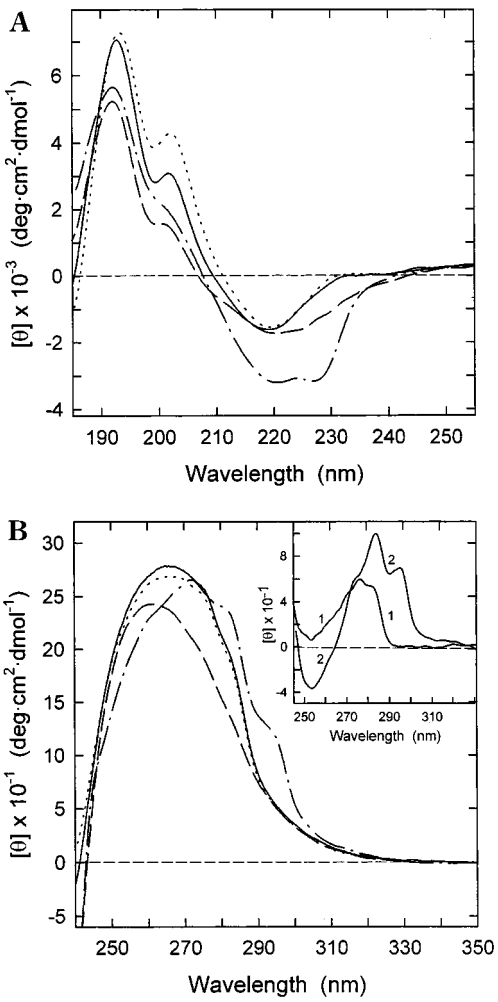

FIGURE 4: Far- (A) and near-UV (B) CD spectra of V1*t*Bug (—), Y3Cha (− −), and Y3αNal (−·−). As a reference, CD spectra of the natural fragment 1−47 (···) are also included. All measurements were carried out at 20 °C in 10 mM sodium phosphate buffer (pH 7.0) at a protein concentration of 20 or 100 μM, in the far- and near-UV regions. The inset shows the difference spectra obtained by subtracting the spectrum of Y3Cha from that of the natural fragment 1−47 (curve 1) or that of the Y3βNal analogue (curve 2).

results of N-terminal sequence analysis (not shown) provided clear-cut evidence that the S2R analogue is not degraded by thrombin. This resistance to proteolytic degradation is in line with the fact that hirudin binds at the active site of thrombin in a nonsubstrate mode (*11*).

Replacement of Tyr3 with the more hydrophobic residues cyclohexylalanine (Cha) and phenylalanine (Phe) enhances binding by 1.6- and 16-fold, respectively. Notably, despite the fact that Cha is more hydrophobic than Phe and possesses roughly the same side chain volume (*23*), the Y3Cha derivative inhibits the fast form of thrombin 10-fold less efficiently than Y3F (see Table 1). In addition, the substitution of Tyr3 with more hydrophobic and bulkier residues such as Trp, αNal, and βNal improves binding to thrombin, with K_d values in the low nanomolar range, and slightly enhances the selectivity of the peptide analogues for the fast form. Interestingly, although αNal and βNal are isosteric and isophobic (*23*), replacement of Tyr3 with βNal leads to a 6-fold increase in binding relative to that of the α-naphthyl isomer (αNal).

Table 1: Thermodynamic Data for the Binding of Synthetic Analogues 1−47 to the Fast and Slow Forms of Thrombin[a]

	fast form		slow form		
synthetic analogue	K_d (nM)	$\Delta\Delta G_b$ (kcal/mol)[b]	K_d (nM)	$\Delta\Delta G_b$ (kcal/mol)[b]	ΔG_c (kcal/mol)[c]
natural	41 ± 2	−	1500 ± 100	−	−2.1
Y3F	2.5 ± 0.2	−1.65	230 ± 10	−1.11	−2.7
Y3Cha	25 ± 2	−0.29	1500 ± 60	0	−2.4
Y3W	6.6 ± 0.7	−1.08	550 ± 40	−0.60	−2.6
Y3αNal	6.4 ± 0.4	−1.10	530 ± 30	−0.62	−2.6
Y3βNal	1.1 ± 0.1	−2.14	94 ± 4	−1.64	−2.6
V1*t*Bug	14 ± 0.4	−0.63	1000 ± 80	−0.24	−2.5
S2R	1.7 ± 0.07	−1.88	12 ±2	−2.86	−1.1

[a] All measurements were carried out at 25 °C in 5 mM Tris (pH 8.0) containing 0.1% PEG in the presence of 200 mM NaCl when the fast form or 200 mM ChCl when the slow form was being studied (see Materials and Methods). [b] $\Delta\Delta G_b$ is the difference in the free energy change of binding to thrombin between the synthetic analogue (ΔG_b*) and the natural fragment (ΔG_b^{wt}): $\Delta\Delta G_b = \Delta G_b^* - \Delta G_b^{wt}$. A negative value of $\Delta\Delta G_b$ indicates that the mutated species binds more tightly to thrombin than the natural fragment. Errors are ±0.1 kcal/mol or less. [c] ΔG_c is the free energy of coupling to thrombin, measured as $\Delta G_c = \Delta G_{b,fast} - \Delta G_{b,slow}$ (*13*, *40*). The value of ΔG_c is negative if the inhibitor binds to the fast form with a higher affinity than it does to the slow form.

DISCUSSION

The major limitation of the protein engineering approach by genetic methods resides in the fact that the structural or functional diversity that can be generated into a given polypeptide chain is limited to the repertoire of the 20 genetically coded amino acids. In this view, the possibility of effectively modulating the physicochemical properties (i.e., hydrophobicity, electronic structure, side chain volume, and shape) of peptide ligands through the rational incorporation of non-natural amino acids with tailored side chains represents a promising approach for studying the determinants of protein folding and stability, as well as for shedding light on the molecular basis of ligand−receptor association (*49*). The most straightforward way of introducing non-natural moieties into proteins is chemical synthesis (*50*), even though other approaches such as enzyme-catalyzed semisynthesis (*51*, *52*) and biosynthetic procedures (*49*) have also been exploited. However, solid-phase peptide synthesis is limited by the peptide chain length (*50*), and in the case of disulfide-containing proteins, the problem is further complicated by the poor recovery of peptide material possessing the correct disulfide bonds.

The results reported in this study demonstrate that it is possible to produce in high yields and in a homogeneous form analogues of fragment 1−47 of hirudin HM2 containing non-natural amino acid residues by combining automated and manual solid-phase peptide synthesis. Moreover, the results of conformational characterization provide evidence that the synthetic peptides retain the overall structure of the natural species, allowing us to interpret the differences in binding to thrombin on the basis of the different physicochemical properties of the mutated residues and of the impact of amino acid exchanges on the structure of the hirudin−thrombin complex. In this respect, it should be pointed out that the structure of thrombin used in this study is that relative to the fast form, since crystallization of the hirudin−thrombin complex was achieved in the presence of 0.2−0.5 M Na^+ (*11*, *12*).

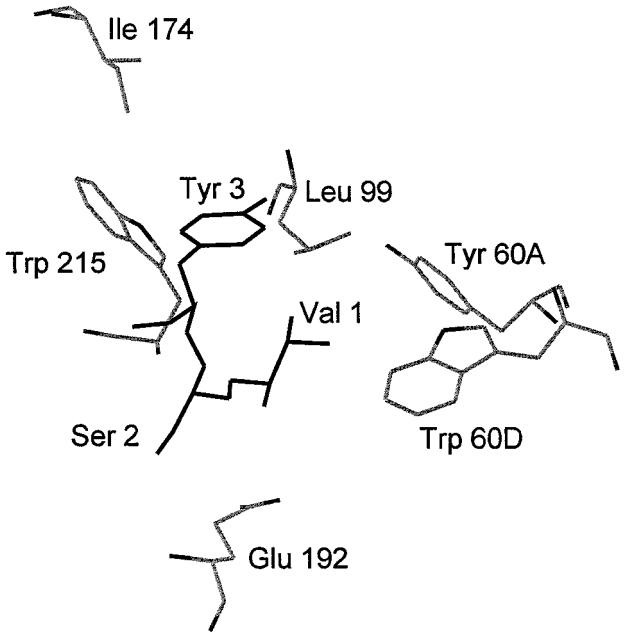

FIGURE 5: Schematic representation of the interaction of the N-terminal tripeptide of hirudin HM2 (black) with the active site of thrombin (gray). The model structure of hirudin HM2 bound to thrombin was based on the coordinates of the X-ray structure (2.3 Å resolution) of the complex between human α-thrombin and the hirudin HV2 variant, possessing an Ile at position 1 and a Val at position 2 (*11*). Only the amino acid side chains of thrombin that interact with the N-terminal tripeptide of hirudin are indicated. For clarity, His57, Asp102, and Ser195 of the active site are not shown. Tyr60A and Trp60D define the S2 site, while Trp215, Leu99, and Ile174 form the apolar binding site (the S3 site) on thrombin. Glu192 of the allosteric core of thrombin (*54*) is also indicated.

Val1 → tBug. As reported in Table 1, replacement of Val1 with *tert*-butylglycine (*t*Bug) enhances the affinity of fragment 1−47 for the fast form of thrombin by about 3-fold, with a gain in the free energy of binding (ΔG_b) of 0.63 kcal/mol. This result is unprecedented, considering that almost all mutations at this position reported so far dramatically decreased binding (*14*, *17*).

Model building studies indicate that *t*Bug can be accommodated at the S2 subsite without steric hindrance and that the improved binding of the V1*t*Bug analogue does not arise from the burial of a larger amount of hydrophobic surface area upon association or from added interactions due to the extra methyl group (see Figure 5). Moreover, the presence of a CH_3 at Cβ of valine is expected to have only a marginal effect in restricting the backbone conformations of fragment 1−47 in the free state, since Val1 is at the N-terminal end of the molecule (see Figure 1). Hence, we propose that the improved binding of V1*t*Bug is due to the higher symmetry of the *tert*-butyl group of *t*Bug compared to that of the isopropyl side chain of Val. NMR data indicate that all three most stable rotamers (trans, gauche$^+$, and gauche$^-$) about χ^1 are observed for the side chain of Val1 in the solution structure of free hirudin (*22*), but only the trans rotamer binds properly to thrombin (*11*, *12*). In the case of *t*Bug, there are three equivalent positions for the three CH_3 groups attached to the β-carbon. This means that there are three energetically equivalent side chain rotamers of *t*Bug that are able to bind thrombin into the functionally active conforma-

tion, leading to a reduction of the entropy change of binding compared to that of Val ($\Delta S_{b,Val\rightarrow tBug}$). An estimate of $\Delta S_{b,Val\rightarrow tBug}$ can be obtained from the equation $\Delta S_{b,Val\rightarrow tBug} = R \ln(\gamma_{b,tBug}/\gamma_{b,Val}) = R \ln(3/1)$ (*53*), where $\gamma_{b,tBug}$ and $\gamma_{b,Val}$ are the number of functionally active conformations allowed for *t*Bug and Val, respectively, in the hirudin−thrombin complex. Thus, a relative stabilization of $\Delta G_{Val\rightarrow tBug}$ which equals $-T\Delta S_{Val\rightarrow tBug}$ (−0.65 kcal/mol at 298 K) is expected for the V1*t*Bug analogue over the natural species, consistent with the experimental value ($\Delta G_{Val\rightarrow tBug} = -0.63$ kcal/mol) reported in Table 1. Our results suggest that proper introduction of symmetric groups into amino acid side chains can significantly improve binding by increasing the entropy of the ligand in the bound state, thus reducing the overall change in ΔS_b. With this respect, amino acid substitutions such as valine → *tert*-butylglycine or leucine → *tert*-butylalanine represent rather safe mutations, enabling improvement in binding with minimal steric requirements.

Ser2 → Arg. Replacement of Ser2 with Arg induces a strong enhancement of the affinity of fragment 1−47 for thrombin (see Table 1), partly anticipated by mutagenesis studies conducted on the full-length hirudin HV1, where Val2 → Arg exchange led to a 9-fold increase in the binding constant (*17*). A reasonable hypotesis, based on molecular modeling studies, suggests that Arg2 of fragment 1−47 may interact with thrombin in a nonsubstrate mode by coupling electrostatically with Glu192 (Cα−Cα distance of ∼5 Å), thereby explaining the higher affinity of the S2R analogue for either the slow or fast form.

The data reported in Table 1 also show that Ser → Arg exchange enhances binding more to the slow form of thrombin than to the fast form. In particular, the S2R analogue binds 24 and 125 times more tightly than the natural species to the fast and slow form of thrombin, respectively, with a difference in coupling free energy (ΔG_c) of 1.0 kcal/mol. The value of ΔG_c measures the difference in ΔG_b between the fast and slow forms ($\Delta G_c = \Delta G_{fast} - \Delta G_{slow}$), and the residues on thrombin that are energetically linked to the slow to fast transition can be mapped from the effect of their mutation on the value of ΔG_c (*13*, *40*). Hence, it may be proposed that Glu192 is involved in the slow to fast transition and that its perturbation by electrostatic coupling to Arg2 in the S2R analogue preferentially stabilizes the slow form of thrombin relative to the natural fragment. This is in line with the results of previous studies conducted by Di Cera and co-workers demonstrating that Glu192 is part of the "allosteric core" of thrombin through which events originating at the Na^+-binding loop propagate to other regions of the enzyme, thus regulating the transition between the slow (anticoagulant) and fast (procoagulant) form (*54*). However, since the direct structural evidence for the binding mode of Arg2 to thrombin is not yet available, our hypothesis awaits structural verification. In this respect, the alternative possibility of Arg2 interacting with Asp189 of thrombin in the S1 cavity can also be considered.

Tyr3 → X. In this study, we have probed the S3 site of thrombin by replacing Tyr3 of hirudin fragment 1−47 with mononuclear (Phe and Cha) and binuclear (Trp, αNal, and *β*Nal) amino acid residues. Thrombin inhibition data reported in Table 1 indicate that the mutated analogues are 2−40-fold more potent than the natural species in inhibiting the fast form, and up to 16-fold more potent than the slow form. Hence, an increase in the hydrophobic character at position 3 of hirudin remarkably improves binding and seems to slightly stabilize the fast form over the slow form, compared to the natural fragment.

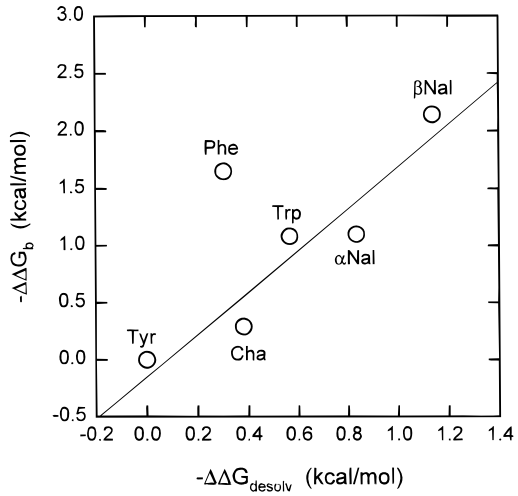

FIGURE 6: Plot of $\Delta\Delta G_b$ vs $\Delta\Delta G_{desolv}$ for the Tyr3 → X analogues of hirudin fragment 1−47. $\Delta\Delta G_b$ is the difference in the free energy change of binding to the fast form of thrombin, as obtained from the experimental data reported in Table 1. $\Delta\Delta G_{desolv}$ is the difference in the desolvation free energy change calculated from the difference in the polar and apolar accessble surface areas (ASA) that become buried upon binding (see Materials and Methods). Both $\Delta\Delta G_b$ and $\Delta\Delta G_{desolv}$ are calculated relative to the natural species. Data points (except that relative to Phe) are fitted to a line with a slope of 1.84, giving a correlation coefficient *r* of 0.95.

Considering the nonpolar character of the mutated side chains, we tried to correlate the free energy change of binding to thrombin (ΔG_b) to the variation of hydrophobicity at position 3. Data reported in Figure 6 clearly indicate that there is a linear proportionality between the experimentally determined ΔG_b and the calculated desolvation free energy of binding (ΔG_{desolv}), mainly contributed by desolvation of apolar surfaces that become buried when hirudin binds to thrombin (see Materials and Methods). These results provide a reasonable physical interpretation for the enhanced inhibitory potency of the synthetic analogues at position 3 and suggest that the hydrophobic effect is an important factor in driving ligand−receptor association. However, the variation of hydrophobicity alone does not account quantitatively for the differences in ΔG_b reported in Table 1. For instance, Y3Cha and Y3F bury approximately the same amount of apolar surface area upon complex formation, and as expected, they have very close desolvation free energies of binding (see Figure 6). Nevertheless, experimental data reported in Table 1 indicate that Y3Cha is 10-fold less active than Y3F, with an unfavorable $\Delta\Delta G_b$ relative to Y3F of 1.36 kcal/mol. Analysis of the 3D structure of the hirudin−thrombin complex indicates that Tyr3 interacts in a favorable edge-to-face conformation with Trp215 at the S3 site of thrombin (*11*, *12*) (see Figure 5), and similar structural features have been observed between D-Phe and Trp215 in the X-ray structure of thrombin complexed with the inhibitor D-Phe-Pro-Arg-chloromethyl ketone (*55*). Aromatic−aromatic interactions have been identified as important factors for protein stability and binding (see ref *56* for a review), since edge-to-face interaction of two aromatic side chains allows the δ^+ hydrogen atoms of the edge of one aromatic ring to

approach the δ^- π-electron cloud of the other ring, leading to a favorable free energy change of interaction between −0.6 and −1.3 kcal/mol (*57*). Hence, in our case, the improved binding of Y3F relative to that of Y3Cha is primarily due to the stabilizing interaction of Phe3 with Trp215, which is possible only for the aromatic side chain of Phe and not for its saturated analogue (Cha).

Experimental data reported in Table 1 reveal that while Trp is less hydrophobic than αNal, as determined by water to octanol transfer data [ΔG_{TR}(Trp) = −3.0 kcal/mol; ΔG_{TR}(α-Nal,βNal) = −4.2 kcal/mol] (*23*), Y3W and Y3αNal display very close antithrombin activities. Conversely, although αNal and βNal have the same hydrophobicity value, Y3βNal is 6-fold more potent than Y3αNal in inhibiting the fast form of thrombin, with a difference in ΔG_b of −1.0 kcal/mol. Model building studies and accessible surface area (ASA) calculations provide a reasonable explanation for these results. In fact, both Trp and αNal have similar side chain orientations and bury approximately the same amount of apolar surface area upon complex formation, giving similar values of ΔG_{desolv} (Figure 6). In addition, Y3W and Y3αNal share a common binding mode, since the aromatic moiety of both Trp and αNal can contact at one end Tyr60A and Trp60D of the S2 site while at the other end can interact edge-to-face with Trp215 of the S3 site (see Figure 5). The improved binding of the Y3βNal analogue relative to that of Y3αNal can be explained by considering the different side chain orientation of α- and βNal (see Figure 2) in the free and bound state. In the free state, the naphthyl ring of βNal protrudes into the aqueous solvent, leading to a larger amount of apolar surface area that is buried upon binding, and thus to an increased value of ΔG_{desolv} (Figure 6). When bound to thrombin, the side chain of βNal does not point toward the S2 site (as in the case of αNal), but it harbors the side chains of Leu99 and Ile174 at the S3 site through favorable van der Waals contacts and interacts edge-to-face with the indole ring of Trp215 (see Figure 5).

An important aspect emerging from this study is that the intrinsic aversion of nonpolar groups for water is the dominant driving force for ligand binding only when the removal of these groups from the aqueous solvent leads to favorable specific interactions with the receptor binding site(s), suggesting that ligand−receptor association is strongly influenced by both hydrophobic and shape-dependent packing effects. If a reasonable estimate of the hydrophobic effect can be obtained by calculating the free energy change due to desolvation of apolar surfaces that become buried upon ligand−receptor association, packing effects are much more difficult to evaluate and predict, since they are mediated by weakly polar interactions (e.g., aromatic−aromatic and van der Waals) whose strength is strongly dependent on the orientation and distance of the interacting groups, such that even subtle perturbations in the ligand or receptor structure may dramatically alter binding.

In summary, the results of this study prove that solid-phase chemical synthesis is a convenient method for the efficient incorporation of non-natural amino acids into the N-terminal domain 1−47 of hirudin, enabling us to obtain analogues more potent than the natural counterpart. Moreover, it is shown that the rational incorporation of non-natural moieties into hirudin can lead to inhibitors that preferentially exert their action on either the procoagulant (fast) or anticoagulant (slow) form of thrombin. Synthetic analogues of hirudin therefore can be used not only to shed light on the molecular recognition phenomenon between thrombin and hirudin but also as anticoagulant agents of potential therapeutic interest.

ACKNOWLEDGMENT

We are grateful to Dr. Gaetano Orsini and Dr. Federico Bertolero (Farmitalia-C. Erba, Milan, Italy) for supplying us with a sample of recombinant hirudin HM2. We thank Dr. Patrizia Polverino de Laureto for mass spectrometry analyses and Dr. Laura Altichieri for performing some of the experiments reported in this study. We also thank Prof. Claudio Toniolo for helpful advice and useful discussions. The excellent technical assistance of Mr. Franco Cavaggion in the use of the peptide synthesizer is also appreciated.

REFERENCES

1. Davie, E. W., Fijikawa, K. A., and Kisiel, W. (1991) *Biochemistry 30*, 10363−10370.
2. Beck, W. S. (1991) in *Hematology* (Beck, W. S., Ed.) MIT Press, Cambridge, MA.
3. Wells, C. M., and Di Cera, E. (1992) *Biochemistry 31*, 11721−11730.
4. Dang, Q. D., Vindigni, A., and Di Cera, E. (1995) *Proc. Natl. Acad. Sci. U.S.A. 92*, 5977−5981.
5. Di Cera, E., Guinto, E. R., Vindigni, A., Dang, Q. D., Ayala, Y. M., Wuyi, M., and Tulinsky, A. (1995) *J. Biol. Chem. 270*, 22089−22092.
6. Berg, D. T., Wiley, M. R., and Grinnell, B. W. (1996) *Science 273*, 1389−1391.
7. Stone, S. R., and Hofsteenge, J. (1986) *Biochemistry 25*, 4622−4628.
8. Folkers, P. J. M., Clore, G. M., Driscoll, P. C., Dodt, J., Kohler, S., and Gronenborn, A. M. (1989) *Biochemistry 28*, 2601−2617.
9. Haruyama, H., and Wütrich, K. (1989) *Biochemistry 28*, 4301−4312.
10. Nicastro, G., Baumer, L., Bolis, G., and Tatò, M. (1997) *Biopolymers 41*, 731−749.
11. Rydel, T. J., Tulinsky, A., Bode, W., and Huber, R. (1991) *J. Mol. Biol. 221*, 583−601.
12. Vitali, J., Martin, P. D., Malkowski, M. G., Robertson, W. D., Lazar, J. B., Winant, R. C., Johnson, P. H., and Edwards, B. F. P. (1992) *J. Biol. Chem. 267*, 17670−17678.
13. Ayala, Y. M., Vindigni, A., Nayal, M., Spolar, R. S., Record, T. M., Jr., and Di Cera, E. (1995) *J. Mol. Biol. 254*, 787−798.
14. Wallace, A., Dennis, S., Hofsteenge, J., and Stone, S. R. (1989) *Biochemistry 28*, 10079−10084.
15. Lazar, J. B., Winant, R. C., and Johnson, P. H. (1991) *J. Biol. Chem. 266*, 685−688.
16. Winant, R. C., Lazar, J. B., and Johnson, P. H. (1991) *Biochemistry 30*, 1271−1277.
17. Betz, A., Hofsteenge, J., and Stone, S. R. (1992) *Biochemistry 31*, 4557−4562.
18. Maraganore, J. M., Bourdon, P., Jablonski, J., Ramachandran, K. L., and Fenton, J. W., II (1990) *Biochemistry 29*, 7095−7101.
19. Lombardi, A., Nastri, F., Della Morte, R., Rossi, A., De Rosa, A., Staiano, N., Pedone, C., and Pavone, V. (1996) *J. Med. Chem. 39*, 2008−2017.
20. De Filippis, V., Vindigni, A., Altichieri, L., and Fontana, A. (1995) *Biochemistry 34*, 9552−9564.
21. Szyperski, T., Güntert, P., Stone, S. R., and Wütrich, K. (1992) *J. Mol. Biol. 228*, 1193−1205.
22. Szyperski, T., Güntert, P., Stone, S. R., Tulinsky, A., Bode, W., Huber, R., and Wütrich, K. (1992) *J. Mol. Biol. 228*, 1206−1211.
23. Fauchère, J.-L., Charton, M., Kier, L. B., Verloop, A., and Pliska, V. (1988) *Int. J. Pept. Protein Res. 32*, 269−278.

24. Lyu, P. C., Sherman, J. C., Chen, A., and Kallenbach, N. R. (1991) *Proc. Natl. Acad. Sci. U.S.A. 88*, 5317−5320.
25. Cornish, V. W., Kaplan, M. I., Veenstra, D. L., Kollman, P. A., and Schultz, P. G. (1994) *Biochemistry 33*, 12022−12031.
26. Paterson, Y., and Leach, S. J. (1978) *Macromolecules 11*, 409−415.
27. Minor, D. L., Jr., and Kim, P. S. (1994) *Nature 367*, 660−663.
28. Steiner, V., Knecht, R., Börsen, K. O., Gasssmann, E., Stone, S. R., Raschdorf, F., Schaleppi, J.-M., and Maschler, R. (1992) *Biochemistry 31*, 2294−2298.
29. De Antoni, F., De Filippis, V., Altichieri, L., Vindigni, A., Polverino de Laureto, P., and Fontana, A. (1996) *Adv. Exp. Med. Biol. 398*, 627−633.
30. Vindigni, A., De Filippis, V., Zanotti, G., Visco, C., Orsini, G., and Fontana, A. (1994) *Eur. J. Biochem. 226*, 323−333.
31. Ten Kortenaar, P. B. W., Van Dijk, B. G., Peeters, M. J., Raabe, B. J., Adams, P. J., and Tesser, G. I. (1986) *Int. J. Pept. Protein Res. 27*, 398−400.
32. Atherton, E., and Sheppard, R. C. (1987) in *The Peptides* (Udenfriend, S., and Meienhofer, J., Eds.) Vol. 9, pp 1−39, Academic Press, New York.
33. Wang, S. S. (1973) *J. Am. Chem. Soc. 95*, 1328−1333.
34. Knorr, R., Trzeciak, A., Bannwarth, W., and Gillessen, D. (1989) *Tetrahedron Lett. 30*, 1927−1930.
35. Chatrenet, B., and Chang, J.-Y. (1992) *J. Biol. Chem. 267*, 3038−3043.
36. Gill, S. G., and von Hippel, P. H. (1989) *Anal. Biochem. 182*, 319−326.
37. Ciardelli, F., Salvadori, P., Carlini, C., Menicagli, R., and Lardicci, L. (1975) *Tetrahedron Lett.*, 1779−1782.
38. Sisido, M., Egusa, S., and Iamanishi, Y. (1983) *J. Am. Chem. Soc. 105*, 1041−1049.
39. Buckler, D. R., Haas, E., and Scheraga, H. A. (1993) *Anal. Biochem. 209*, 20−31.
40. Ayala, Y. M., and Di Cera, E. (1994) *J. Mol. Biol. 235*, 733−746.
41. Horton, N., and Lewis, M. (1992) *Protein Sci. 1*, 169−181.
42. Juffer, A. H., Eisenhaber, F., Hubberd, S. J., Walther, D., and Argos, P. (1995) *Protein Sci. 4*, 2499−2509.
43. Eisenberg, D., and McLachlan, A. D. (1986) *Nature 319*, 199−203.
44. Richards, F. R. (1985) *Methods Enzymol. 115*, 440−464.
45. Brahms, S., and Brahms, J. (1980) *J. Mol. Biol. 138*, 149−178.
46. Kahn, P. C. (1979) *Methods Enzymol. 61*, 339−378.
47. Strickland, E. H. (1974) *CRC Crit. Rev. Biochem. 3*, 113−175.
48. Perona, J. J., and Craik, C. S. (1995) *Protein Sci. 4*, 337−360.
49. Mendel, D., Cornish, V. W., and Schultz, P. G. (1995) *Annu. Rev. Biomol. Struct. 24*, 435−462.
50. Kent, S. R. H. (1988) *Annu. Rev. Biochem. 57*, 957−989.
51. Wallace, C. J. A. (1993) *FASEB J. 7*, 505−515.
52. De Filippis, V., De Antoni, F., Frigo, M., Polverino de Laureto, P., and Fontana, A. (1998) *Biochemistry 37*, 1686−1696.
53. Wang, J., Szewczuk, Z., Yue, S.-Y., Tsuda, Y., Konishi, Y., and Purisima, E. O. (1995) *J. Mol. Biol. 253*, 473−492.
54. Guinto, E. R., Vindigni, A., Ayala, Y. M., Dang, Q. D., and Di Cera, E. (1995) *Proc. Natl. Acad. Sci. U.S.A. 92*, 11185−11189.
55. Bode, W., Turk, D., and Karshikov, A. (1992) *Protein Sci. 1*, 426−472.
56. Burley, S. K., and Petsko, G. A. (1988) *Adv. Protein Chem. 39*, 125−189.
57. Burley, S. K., and Petsko, G. A. (1985) *Science 229*, 23−28.
58. Scacheri, E., Nitti, G., Valsasina, B., Orsini, G., Visco, C., Ferreia, M., Sawyer, R. T., and Sarmientos, P. (1993) *Eur. J. Biochem. 214*, 295−304.
59. Kraulis, P. J. (1991) *J. Appl. Crystallogr. 24*, 946−950.

BI980717N